22nd Course of the International School of Geophysics
ERMES - EARTHQUAKE MECHANICS, EARTH STRUCTURE AND RELATED PROBLEMS
EMCSC, Erice, Sicily, 1 - 8 August, 2002

Fault Constitutive Properties and Earthquake Interactions

Massimo Cocco, Andrea Bizzarri & Elisa Tinti
Istituto Nazionale di Geofisica e Vulcanologia (Rome, Department Seismology and Tectonophysics)

Constitutive laws govern fault friction during the nucleation and propagation of earthquake ruptures and are required to have a finite fracture energy absorbed at the crack tip. The relation between the adopted friction law and the total dynamic traction represents one of the fundamental equations to be solved to model spontaneous dynamic ruptures. Fault friction controls the dynamic process during a single rupture episode, the earthquake repetition during the seismic cycle and earthquake triggering mechanisms due to stress interactions. In the literature two main classes of constitutive formulations have been proposed: the slip–dependent and the rate– and state–dependent (R&S) friction laws. The former assumes that friction only depends on slip, while the latter considers that friction depends on slip velocity and state variables. The first class of constitutive models includes the "classical" slip–weakening (SW) law (Barenblatt, 1959; Ida, 1972; Palmer and Rice, 1973; Andrews, 1976a, b), although other modified slip–weakening behaviors have been proposed that include a slip–hardening phase and an exponential decrease of traction with displacement (see Ohnaka, 1996 and references therein). The second class of constitutive equations is based on the laboratory derived friction laws, which were originally proposed by Dieterich (Dieterich, 1979, 1986, 1992; Ruina 1983). These two constitutive formulations can both be applied to model a dynamic crack propagation (see Bizzarri et al., 2001 and references therein), but they provide a completely different description of the nucleation process (see Dieterich, 1992; Onhaka and Shen, 1999). Further modifications of these constitutive laws have been also proposed to model the rupture healing and to control the slip duration during dynamic rupture propagation (see Beeler and Tullis, 1996; Zheng and Rice, 1998 and references therein). The main difference between slip and rate & state constitutive formulations concerns the time dependence of friction: in fact only rate– and state–dependent friction laws consider an evolution equation for the state variable that yields a time dependency of friction and accounts for fault restrengthening. Therefore, R&S laws are suitable to model the faulting process and repeated slip episodes on the fault plane.

Dynamics of individual ruptures. The slip–weakening behavior describes the traction drop associated to slip acceleration, which is a consequence of a dynamic failure process. Slip weakening is a characteristic feature of rate and state constitutive laws (Okubo and Dieterich, 1984; Cocco and Bizzarri, 2002). This process occurs at the crack tip in a finite extended zone named the cohesive zone (Ida, 1972; Andrews, 1976a, b; Ohnaka, 1989; see Figure 1). Therefore, these two constitutive laws should not be considered as alternative, at least to describe the dynamic propagation during a single rupture event. However, an important question arising from these considerations is what

controls the slip weakening behavior within the cohesive zone, or which are the physical processes controlling the evolution of the dynamic traction and the consequent slip acceleration during the breakdown process. Healing mechanisms controlling the slip deceleration and duration are also associated to the weakening process (Beeler and Tullis, 1996; Zheng and Rice, 1998). Adopting a SW law implicitly implies that the traction evolution in the cohesive zone is prescribed. This represents the most important phenomenon to be considered to model earthquake rupture propagation and the genesis of seismic waves (see for instance Fukuyama and Madariaga, 1998). In the framework of R&S constitutive laws slip–weakening might be considered as the result of a physical process associated to the frictional control of dynamic rupture growth. In this lecture we aim to answer to these questions. According to these considerations it is clear that, in order to simulate the dynamic rupture propagation during a single earthquake (see Olsen et al., 1997, Fukuyama and Madariaga, 1998, among different others) with spontaneous models, the adoption of a SW law has the important advantage to prescribe the dynamic traction evolution within the cohesive zone. This is exactly what is needed to allow the crack to advance, the rupture to propagate and to generate seismic waves. However, this does not answer to the questions proposed before on the origin of weakening processes.

Methodology. In this work we solve the elasto–dynamic fundamental equation

$$\rho\,\ddot{u}_i = \sigma_{ij,j} + f_i \tag{1}$$

for a 2–D in–plane shear crack for which the displacement and the shear traction depend on time and on only one spatial coordinate; we also neglect the body forces ($f_i = 0$). In (1) r is the mass density, u the displacement and $s_{ij,j}$ is the spatial derivative of the stress tensor components. In particular, we assume that the crack propagates only in the x_1–direction and the fault surface is the $x_3 = 0$ plane. The medium is supposed to be infinite, homogeneous and elastic everywhere except along the fracture line. We solve equation (1) by using a finite difference (FD) approach described in Andrews (1973) and Andrews and Ben–Zion (1997). A grid of nodes is introduced and each node is a vertex of an equilateral triangle; the slip velocity components are staggered in both space end time with respect to the total shear stress components S_{ij}. The latter are defined in the centre of the triangles and at integer time steps, while the first ones are defined in the vertexes of the triangles and at intermediate time steps:

$$\begin{aligned} r\,\frac{\partial}{\partial t}\dot{u}_1 &= \frac{\partial}{\partial x_1}\Sigma_{11} + \frac{\partial}{\partial x_2}\Sigma_{12} \\ r\,\frac{\partial}{\partial t}\dot{u}_2 &= \frac{\partial}{\partial x_1}\Sigma_{12} + \frac{\partial}{\partial x_2}\Sigma_{22} \end{aligned} \tag{2}$$

The details of the numerical solution are described in Bizzarri et al. (2001). We can use in our procedure either R&S laws with slowness (ageing) evolution equation (Dieterich, 1986):

$$\tau = \left[\mu_* - a\ln\left(\frac{v_*}{v}+1\right) + b\ln\left(\frac{\Phi\, v_*}{L}+1\right)\right]\sigma_n^{\,eff} \tag{3a}$$

$$\frac{\mathrm{d}}{\mathrm{d}t}\Phi = 1 - \frac{\Phi\, v}{L} \tag{3b}$$

or with slip evolution equation (Beeler et al., 1994; Roy and Marone, 1996)

$$\begin{cases} t = \left[m_* - a \ln\left(\frac{v_*}{v} \right) + b \ln\left(\frac{J v_*}{L} \right) \right] s_n^{eff} \\ \frac{\mathrm{d}}{\mathrm{d}t} J = \frac{J v}{L} \ln\left(\frac{J v}{L} \right) \end{cases} \tag{4}$$

We can also use a slip weakening law as introduced by Andrews (1976a, b):

$$\tau = \begin{cases} \tau_u - (\tau_u - \tau_f) \frac{u}{d_0} & , u < d_0 \\ \tau_f & , u \geq d_0 \end{cases} \tag{5}$$

In (3) v is the slip velocity, F is the state variable, m_* and v_* are arbitrary reference values for the friction coefficient and for the slip velocity, respectively; a, b and L are the three constitutive parameters. In this formulation the state variable has the physical meaning of an average contact time between the sliding surfaces (Dieterich, 1986; Ruina, 1983). The evolution equation (3b) is the slowness law (Ruina, 1983; Beeler et al., 1994; Roy and Marone, 1996), and it includes true ageing. In this work we consider a velocity weakening behavior (that is, $B > A$). The slip evolution law is defined in (4). In (5) t_0 is the initial stress (or pre−stress), t_u is the upper yield stress, t_f is the final, kinetic friction level and d_0 is the characteristic slip−weakening distance. The characteristic length scale parameters of these two constitutive formulations are the slip weakening distance d_0 and the parameter L: the former represents the slip required for traction to drop, the latter is the characteristic length controlling the evolution of the state variable. In a recent paper Cocco and Bizzarri (2002) have investigated the slip weakening behavior of rate− and state− constitutive laws and have shown that these two length scale parameters are different. They propose a scaling law between d_0 and L valid for a slowness evolution law, which states that their ratio is nearly 15. In the present study we aim to investigate in greater detail how the constitutive parameters control the slip weakening behavior in the framework of R&S dependent laws and to provide a theoretical explanation of the numerical results.

Modeling results. Figure 1 shows that in a homogeneous configuration using a R&S constitutive formulation the cohesive zone shrinks during the dynamic rupture propagation, as also observed for the classic SW law by Andrews (1976a, b). The resulting time histories of slip, slip velocity and total dynamic traction are, as expected, very similar to those obtained in numerical simulations which adopt the classic SW laws (see comparisons in Bizzarri et al., 2001). However, the analysis of total dynamic traction as a function of slip velocity and slip reveals that velocity–hardening and –weakening clearly exist, and the resulting SW curves are very similar to the generally adopted classic laws (see Figure 2). A characteristic slip–weakening distance exists also for the R&S friction formulation (Okubo and Dieterich, 1986). This is not surprisingly because the slip increase occurs while total dynamic traction decreases yielding slip–weakening.

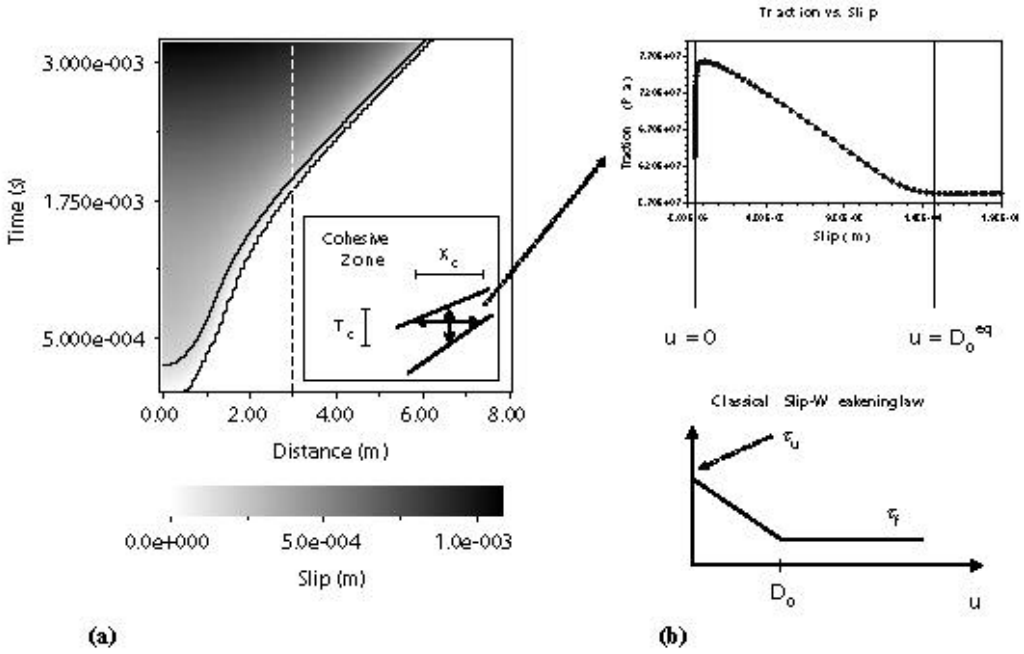

Figure 1. (a) Spatio–temporal evolution of slip for a 2–D in–plane crack: The gray scale shows the slip amplitudes as a function of time and spatial position. The black lines depict the cohesive zone where the total dynamic traction drops from the maximum yield stress to the kinetic friction (as shown in **(b)** for a point located at x = 3.0 m, dashed line). The box inserted in panel (a) depicts a zoom of the cohesive zone: T_c is the duration and X_c is the spatial extension of the cohesive zone. A SW behavior occurs within the cohesive zone also when a R&S constitutive law is adopted and it results very similar to the classical theoretical law **(see panel b).** The adopted constitutive parameters are: $l = m$ = 27 GPa, V_P = 5196 m/s, V_S = 3000 m/s, m_* = 0.56, s_n = 100 MPa, a = 0.012, b = 0.016, L = 10 μm, V_i = 10 μm/s.

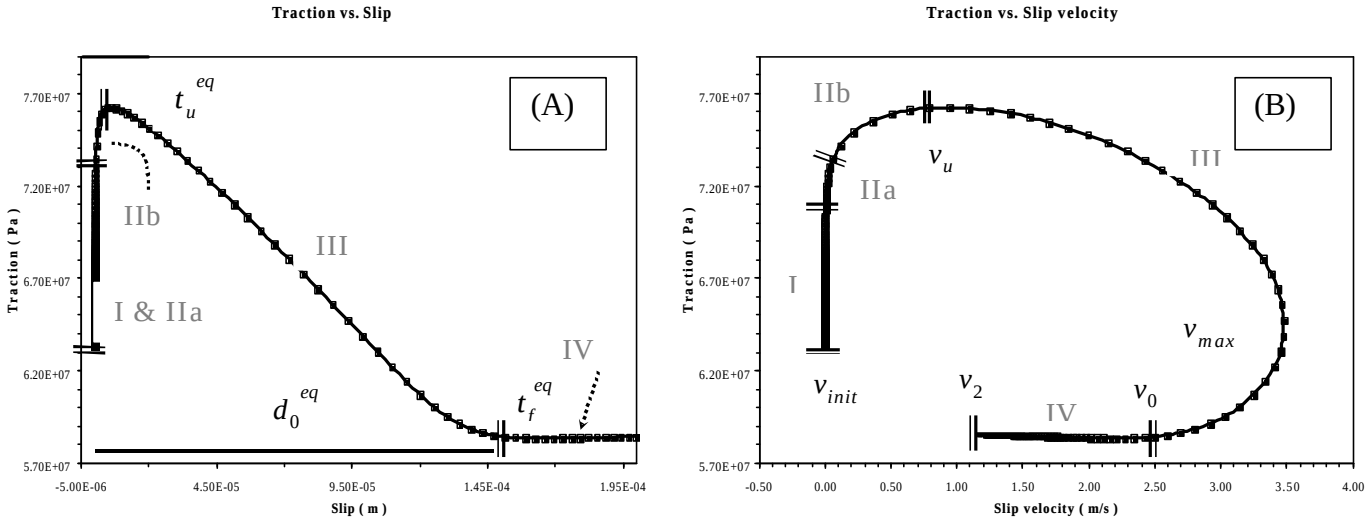

Figure 2. Behavior of traction vs. slip **(a)** and phase diagram (i. e. traction vs. slip rate; **b**) in the fault point x_1 = 3.0 m for a propagating rupture obeying to Dieterich–Ruina law. In both the panels we indicate the different stages of the breakdown process the equivalent frictional parameters for the SW the slip–weakening formulation.

The important question is what controls the SW behavior in the R&S formulation. Our numerical simulations show that, when the propagating rupture front approaches the target grid point, the dynamic stress increases due to the direct effect of friction, although the growth of slip velocity is quite slow at the beginning (phase I in Figure 2). When the dynamic traction is reaching

its maximum value (the yield stress) the slip velocity suddenly increases (phase II); this acceleration phase begins when the total dynamic traction is close to the peak yield stress. The subsequent traction drop coincides with the SW phase and slip velocity reaches its maximum value (phase III). The acceleration from the initial to the peak slip velocity is very fast and occurs in an extremely short time (see Figure 3). Finally, the dynamic traction reaches the kinetic friction level and slip velocity decreases to the new steady state value. The analysis of the 3D phase trajectories represented in Figure 4 shows that SW occurs when the acceleration stage is already started. It is the evolution of the state variable within the cohesive zone from its initial value to the final one that drives the slip acceleration and the fast approaching to the peak slip velocity. This evolution occurs within the cohesive zone when the rupture propagation is initiated and fully dynamic; it has nothing to do with the nucleation process and it happens well before of the eventual healing phases. It is clear that during the dynamic slip the total traction depends on slip, slip velocity and the state variable [Madariaga and Cochard, 1996], although the adopted constitutive formulation only requires the analytical dependence on slip velocity and state. Several authors adopted a rate– and slip–weakening friction in a theoretical way (Madariaga et al., 1998, Fukuyama and Madariaga, 1998). We have shown, however, that hardening effects clearly exist and the state variable evolution controls the traction behavior and the slip acceleration.

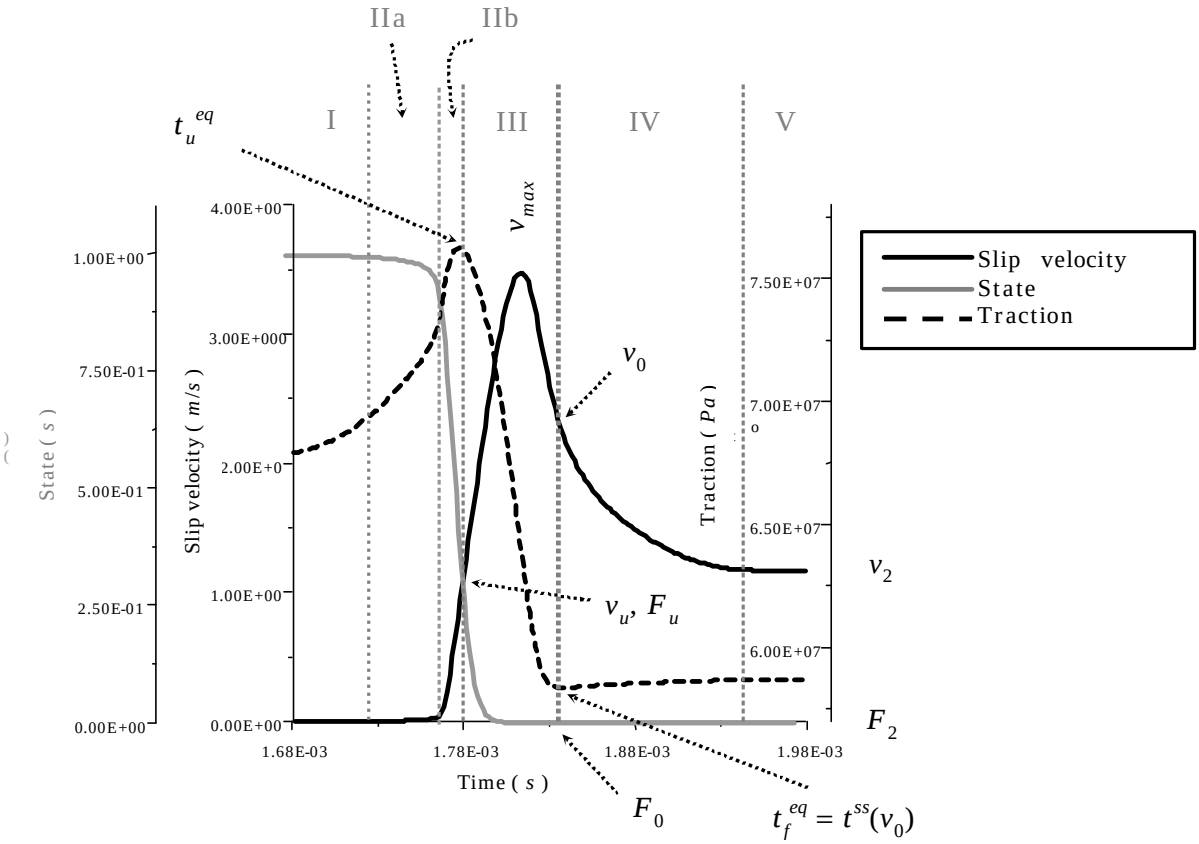

Figure 3. Superposition of the state, slip velocity and traction histories in the same fault point and for the same configuration of Figure 1. We indicate all the stages of the dynamic rupture to emphasize that the state evolution controls the increase of slip velocity and fault friction. v_u is the slip velocity value reached when the traction is at its maximum value (t_u^{eq}); v_0 is the value when the fault has slipped of an amount equal to d_0^{eq} and v_2 is the final value of slip rate.

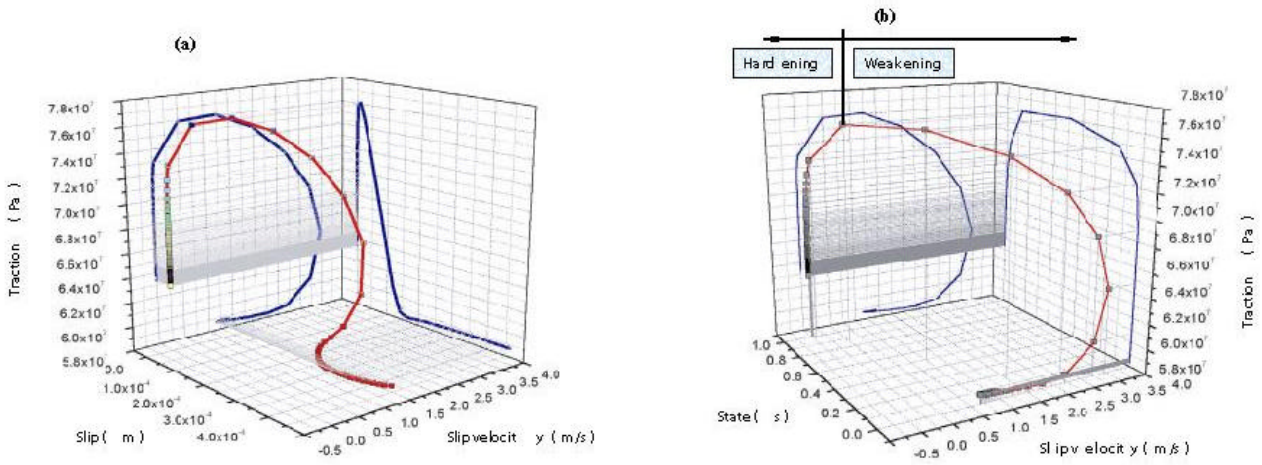

Figure 4. 3–D phase diagrams showing total dynamic traction as a function of slip and slip velocity **(a)** and state and slip velocity **(b)**. The projections of the 3–D trajectories on the vertical planes show the expected behaviors for slip–weakening, velocity–hardening and –weakening as well as the state variable evolution within the cohesive zone. In (b) the state evolves from the initial steady state (L/V_i) up to the final, new steady state (L/V_0).

Physical Interpretation. SW is intrinsic in R&S laws, but the characteristic slip–weakening distance does not coincide with L, which is the characteristic length parameter of this dynamic formulation. We define this slip–weakening distance resulting from R&S laws as an equivalent value D_0^{eq}. The fast evolution of slip velocity represents a serious limitation to retrieve and constrain the constitutive behavior and parameters within the cohesive zone by inverting recorded seismograms (see Guatteri et al., 2001; Cocco and Bizzarri, 2002). In order to understand the evolution of dynamic traction within the cohesive zone and to identify the physical quantities controlling the SW behavior, we compare the time histories of total traction, slip velocity and state variable (Figure 3) calculated for the same model parameters used in Figure 1 (i. e. the reference case) in the same fault position ($x_1 = 3.0\ m$). By looking at Figure 3 it emerges that the resulting total dynamic traction reaches its peak value (the yield stress) earlier than slip velocity, and that the state variable evolves from its initial steady state value to a final one well before the other two. This corroborates our conclusion that is the state variable that drives the slip acceleration and the traction drop during the weakening phase. We have indicated in Figure 3 the five distinct stages comprising the duration of the whole breakdown process. Attempts in constraining the critical slip–weakening distance by means of dynamic consistent waveform inversions (Ide and Takeo, 1997; Guatteri and Spudich, 2000), as well as forward 3D dynamic modeling (Olsen et al., 1997), yield values larger than 0.2 *m*. We do not discuss here the required resolution to constrain the slip–weakening distance from recorded seismograms. We point out, however, that these large values might be caused by smearing effects due to the lack of resolution of the cohesive zone dimension. Moreover, if these large values are real, they would imply nucleation patches ranging between few to tens of kilometers, sometimes reaching 50% of the whole fault length (see for instance Voisin et al., 2001). We have performed many numerical simulations using different values of L and keeping constant

the others constitutive parameters. The results of these calculations are shown in Figure 5. The slip–weakening curves plotted in this figure point out the dependence of D_o^{eq} on L: the equivalent slip–weakening distance resulting from the R&S dependent law here considered is larger than the adopted L value and it increases for increasing L. Moreover, we emphasize that D_o^{eq} also depends on the other constitutive parameters a and b, since they control the yield stress and the kinetic friction. We will discuss this in this lecture.

d_0^{eq} (modeled)	d_0^{eq} (approx.)	d_0^{eq} (modeled)/L
8.36e–5 *m*	6.11e–5 *m*	16.72
1.52e–4 *m*	1.22e–4 *m*	15.20
1.69e–4 *m*	1.34e–4 *m*	15.37
1.80 e–4 *m*	1.83 e–4 *m*	12.00
2.00 e–4 *m*	2.32 e–4 *m*	10.52

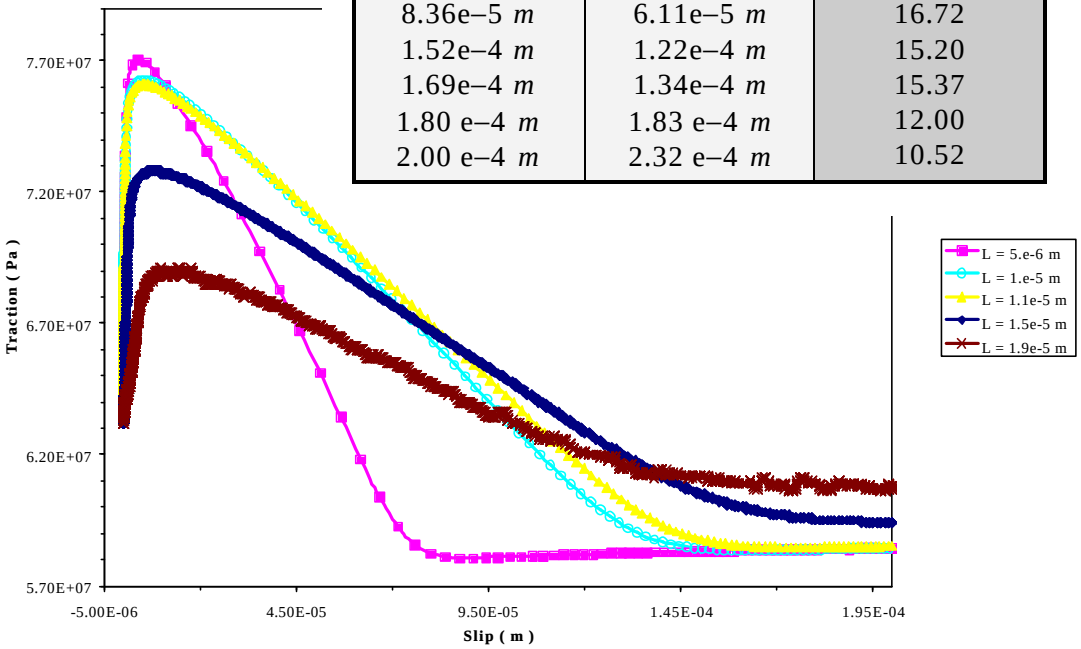

Figure 5. Slip weakening curves for different values of the parameter *L*.

The state variable evolution controls both the friction increase and decrease and the consequent slip acceleration and it involves proportionality between the critical slip weakening distance (D_o^{eq}) and *L*. We have derived a scaling law between *L* and D^0_{eq}.

$$D_0^{eq} = L \ln\left(\frac{V_0}{V_i}\right) \approx \frac{t_u^{eq} - t_f^{eq}}{b\, s_n} L \qquad (2)$$

where τ_u^{eq} and τ_f^{eq} represent the yield and the kinetic stress values for the R&S constitutive formulation. The proportionality factor between these two length parameters scales with the dynamic stress drop and the constitutive parameters. The dependence on *L* is quite simple, but the effect of the other constitutive parameters a and b is more complex since they also affect the yield stress and the kinetic friction. We will present however analytical relations for the yield stress and the kinetic friction that are useful to associate R&S to SW constitutive parameters. The theoretical relation proposed above shows that the equivalent slip–weakening distance D_o^{eq} depends on the initial value of slip velocity, which controls the initial steady–state value of the state variable. The proposed scaling between D_o^{eq} and the dynamic stress drop is an approximated relation: the

calculated D^0_{eq} values slightly underestimate those resulting from numerical simulations. Because the initial slip velocity is totally arbitrary, it is difficult in the framework of R&S formulation to prescribe the traction evolution and the SW behavior within the cohesive zone. We can only infer an approximated value of the equivalent slip–weakening distance from the proposed scaling law. Moreover, the difference between these two length scale parameters depends on the adoption of a slowness (ageing) evolution equation. Preliminary results indicate that a slip evolution equation does not provide similar values for D^0_{eq} and the scaling with L is different. We will discuss in this lecture the implications for scaling from laboratory to earthquake fault dimensions as well as for fracture energy.

Implications for rupture healing. We have shown that the evolution law and the state variable controls the traction drop during slip acceleration (i.e. the SW behavior). It is important to remark that the SW resulting from our simulations is very similar to the theoretical law and shows a nearly linear traction decay corresponding to a constant weakening rate. The conclusion that the state variable evolution controls the breakdown process has important implications also on the mechanisms responsible for rupture healing (i.e. the total slip duration in a fixed point of the fault). Beeler and Tullis (1996) and Zheng and Rice (1998) have discussed this problem in detail. Here we show several numerical results aimed to the definition of the direct effect of friction (intrinsic in R&S) and in particular to its effect on weakening and healing processes. We will show the results of several numerical simulations showing how the state variable evolution control the breakdown process.

Implication for repeated earthquake ruptures and fault interaction. The adoption of rate and state dependent laws has also important implication for fault interaction and earthquake triggering. We will discuss in this lecture how this affect the rate of earthquake production and which are the important implications for fault interaction. This constitutive approach relies on the earthquake nucleation model associated to the rate and state friction formulation. We will discuss the limitations of this approach and the perspectives to evaluate the earthquake after-effects and the modifications to the seismicity rates in the area surrounding the causative fault.

References

Andrews, D. J., 1973. A numerical study of tectonic stress release by underground explosions. Bull. Seism. Soc. Am. 63, No. 4, 1375 – 1391

Andrews, D. J., 1976a. Rupture propagation with finite stress in antiplane strain. J. Geophys. Res. 81, No. 20, 3575 – 3582

Andrews, D. J., 1976b. Rupture velocity of plane strain shear cracks. J. Geophys. Res. 81, No. 32, 5679 – 5687

Andrews, D. J., 1985. Dynamic plane – strain shear rupture with a slip–weakening friction law calculated by a boundary integral method. Bull. Seism. Soc. Am. 75, No. 1, 1 – 21

Andrews, D. J., Ben– Zion Y., 1997. Wrinkle–like slip pulse on a fault between different materials. J. Geophys. Res. 102, No. B1, 553 – 571

Barenblatt, G. I., 1959. Concerning equilibrium crack forming during brittle fracture. The stability of isolated cracks. Relationship with energetic theories. Appl. Math. Mech. 23, 1273 – 1282

Beeler, N. M., Tullis T. E. 1996. Self–healing slip pulses in Dynamic rupture models due to velocity–dependent strength. Bull. Seism. Soc. Am. 86, No. 4, 1130 – 1148

Beeler, N. M., Tullis T. E., Weeks J. D., 1994. The roles of time and displacement in the evolution effect in rock friction. Geophys. Res. Lett. 21, No. 18, 1987 – 1990

Bizzarri, A., Cocco M., Andrews D. J., Boschi E., 2001. Solving the dynamic rupture problem with different numerical

approaches and constitutive laws. Geophys. J. Int. 144, 656 – 678
Boatwright, J., Cocco M., 1996. Frictional constraints on crustal faulting. J. Geophys. Res. 101, No. B6, 13895 – 13909
Cocco, M., Bizzarri A., 2002. On the slip–weakening behavior of rate– and state–dependent constitutive laws. Geophys. Res. Lett. 29, No. 11, 1 – 4
Das, S., Aki K., 1977a. A numerical study of two–dimensional spontaneous rupture propagation. Geophys. J. Roy. Astr. Soc. 50, 643 – 668
Das, S., Aki K., 1977b. Fault plane with barriers: a versatile earthquake model. J. Geophys. Res. 82, No. 36, 5658 – 5670
Dieterich, J. H., 1979. Modeling of rock friction–1. Experimental results and constitutive equations. J. Geophys. Res. 84, 2161 – 2168
Dieterich, J. H., 1986. A model for the nucleation of earthquake slip. Earthquake Source Mechanics, Geophysical Monograph. 37. Maurice Ewing Series, 6, edited by S. Das, J. Boatwright and C. H. Scholz. Am. Geophys. Union. Washington D. C., 37 – 47
Dieterich, J. H., B. Kilgore, 1994. Direct observations of frictional contacts: new insights for state–dependent properties. Proc. Natl. Acad. Sci. USA. 93, 283 – 302
Fukuyama, E., Madariaga R., 1998. Rupture dynamics of a planar fault in a 3–D elastic medium: rate– and slip–weakening friction. Bull. Seism. Soc. Am. 88, No. 1, 1 – 17
Guatteri, M., Spudich P., 2000, What can strong–motion data tell us about slip–weakening fault–friction laws?. Bull. Seism. Soc. Am.. 90, No. 1, 98 – 116
Guatteri, M., Spudich P., Beroza G. C., 2001. Infering rate and state friction parameters from rupture model of the 1995 Hyogo–ken Nambu (Kobe) Japan earthquake. J. Geophys. Res. (in press)
Ida, Y., 1972. Cohesive force across the tip of a longitudinal–shear crack and Griffith' s specific surface energy. J. Geophys. Res.. 77, 3796 – 3805
Ide, S., Takeo M., 1997. Determination of constitutive relations of fault slip based on seismic wave analysis. J. Geophys. Res. 102, No. B12, 27379 – 27391
Madariaga, R., Cochard A., 1996. Dynamic friction and the origin of the complexity of earthquake sources, Proc. Natl. Acad. Sci. USA, 93, 3819 – 3824, Colloquium paper
Madariaga, R., Olsen K., Archuleta R., 1998. Modeling dynamic rupture in a 3 D earthquake fault model, Bull. Seism. Soc. Am., 88, No. 5, 1182 – 1197
Marone, C. J., 1998. Laboratory–derived friction laws and their application to seismic faulting. Annu. Rev. Earth Planet Sci. 26, 643 – 696
Ohnaka, M., 1996. Nonuniformity of the constitutive law parameters for shear rupture and quasistatic nucleation to dynamic rupture: a physical model of earthquake generation processes. Proc. Natl. Acad. Sci. USA. 93, 3795 – 3802
Ohnaka, M., Shen L. F. 1999. Scaling of the shear rupture process from nucleation to dynamic propagation: implications of geometric irregularity of the rupturing surfaces. J. Geophys. Res. 104, 817 – 844
Okubo, P. G., 1989. Dynamic rupture modeling with laboratory–derived constitutive relations. J. Geophys. Res. 94, No. B9, 12321 – 12335
Okubo, P. G., Dieterich J. H., 1984. Effects of physical fault properties on frictional instabilities produced on simulated faults. J. Geoph. Res. 89, 5817 – 5827
Olsen, K. B., Madariaga R., Archuleta R. J. 1997. Three–dimensional dynamic simulation of the 1992 Landers earthquake. Science. 278, 834 – 838
Olsen, K. B., Fukuyama E., Mikumo T., 2001. Direct measurement of the slip weakening distance from near–fault strong motion data. Proc. AGU Fall Meeting
Palmer, A. C., Rice J. H., 1973. The grow of slip surfaces in the progressive failure of over consolidated clay. Proc. R. Soc. London Ser. A 332, 527 – 548
Roy, M., Marone C., 1996. Earthquake nucleation on model faults with rate– and state–dependent friction: effects of inertia. J. Geoph. Res. 101, 13919 – 13932
Ruina, A. L., 1983. Slip instability and state variable friction laws, J. Geophys. Res. 88, No. B12, 10359 – 10370
Voisin, C., Campillo M., Ionescu I. R., Cotton F. and O. Scotti, 2001. Dynamic versus static stress triggering and friction parameters: inferences from the November 23, 1980 Irpinia earthquake, J. Geophys. Res.
Zheng, G., Rice J. R., 1998. Conditions under which velocity–weakening friction allows a self–healing versus a cracklike mode of rupture. Bull. Seism. Soc. Am. 88, No. 6, 1466 – 1483